Research Square

Preprints are preliminary reports that have not undergone peer review.
They should not be considered conclusive, used to inform clinical practice,
or referenced by the media as validated information.

Integrated transcriptomic and co-expression network analysis reveals key transcription factors regulating salt stress responses in rice seedling roots

yimei Zou
Guangdong Academy of Agricultural Sciences
tengkui Chen
Guangdong Academy of Agricultural Sciences
hao Liu
Crops Research Institute, Guangdong Academy of Agricultural Sciences
Muhammad J. Umer
Crops Research Institute, Guangdong Academy of Agricultural Sciences
Sunil S. Gangurde
CIMMYT-China Shandong Wheat and Maize Research Center
dilin Liu
Guangdong Academy of Agricultural Sciences
wuge Liu
Guangdong Academy of Agricultural Sciences
feng Wang
Guangdong Academy of Agricultural Sciences
xing Huo
huox@gdaas.cn

Guangdong Academy of Agricultural Sciences

Research Article

Keywords: rice, salt stress, transcriptome sequencing, rice roots, transcription factor

Posted Date: May 27th, 2026

DOI: https://doi.org/10.21203/rs.3.rs-9628301/v1

License: This work is licensed under a Creative Commons Attribution 4.0 International License.
Read Full License

Additional Declarations: No competing interests reported.

Abstract

Background

Soil salinization severely affects rice growth and yield particularly at the seedling stage. Understanding the molecular mechanisms underlying salt tolerance is therefore crucial for developing salt tolerant cultivars. In this study, gradient NaCl concentrations were applied and phenotypic analysis combined with transcriptome sequencing was conducted to systematically investigate salt stress responses in rice seedling roots.

Results

Phenotypic results showed that salt stress significantly inhibited seedling growth, including primary root, lateral root, and shoot development, with inhibition intensifying as NaCl concentration increased. Transcriptome analysis identified 30,910 expressed genes, among which 7,687 were differentially expressed genes (DEGs). Integration of DEG analysis with weighted gene co-expression network analysis (WGCNA) further identified 5,591 key module genes. Co-expression network analysis revealed 89 hub genes and 99 transcription factor-related genes, highlighting complex regulatory interactions under salt stress. Functional enrichment analysis indicated that low salt stress primarily affected pathways related to osmotic adjustment and ion transport, whereas high salt stress activated pathways associated with secondary metabolism, glutathione metabolism, and stress signaling. A total of 299 common DEGs were identified as core components of the salt stress response. Further analysis identified 10 core transcription factors belonging to the bHLH, NAC, ERF, WRKY, and MYB families. Among them, *OsNAC1*, *OsNAC10*, and *OsNAC15* were determined to be key candidate regulators. Functional validation using mutant lines demonstrated that loss of these genes significantly impaired root growth under salt stress.

Conclusions

This study systematically elucidates gene expression patterns, regulatory networks, and key pathways involved in salt stress responses in rice seedling roots, providing important insights into the molecular basis of salt tolerance and valuable candidate genes for molecular breeding.

1. Introduction

Salinization resulting from excessive soil salt accumulation is a major abiotic stressor that constrains crop growth, development, seed germination, and yield formation, posing a severe threat to the sustainability of global crop production[1, 2]. Currently, approximately 20%~30% of the world's 230 million hectares of irrigated land are affected by salinization to varying extents, and this proportion continues to rise due to human activities such as land reclamation and agricultural irrigation [3]. Notably,

rice exhibits high sensitivity to salt stress at the seedling stage, a trait that frequently leads to yield reduction or even plant mortality [4]. Therefore, to mitigate the constraints of salt stress on rice production, characterizing salt tolerance-related regulatory genes in rice and deciphering their underlying mechanisms have become a core research focus in the field of crop stress resistance molecular biology.

In recent years, through the in-depth integration of model plant and crop research in the field of plant salt tolerance, a robust research framework has been developed, encompassing basic theoretical analysis, gene resource exploration, and breeding technology translation. As a classic model plant, *Arabidopsis* has provided a core theoretical basis for unraveling the mechanisms underlying plant salt tolerance. Studies have confirmed that overexpression of the *SOS1* gene, encoding a plasma membrane Na^+/H^+ antiporter, markedly enhances salt tolerance in *Arabidopsis* [5]. Furthermore, photoactivated phyA and phyB positively regulate the salt tolerance response in Arabidopsis by promoting SOS2-mediated phosphorylation and the degradation of *PIF1* and *PIF3* [6]. These studies have uncovered the conserved molecular mechanisms governing plant salt stress responses, offering important theoretical references for the identification and functional characterization of salt tolerance genes in rice.

In rice, homologous genes of the SOS family are present and exert crucial regulatory functions in salt tolerance. *OsSOS1*, the rice homolog of *SOS1*, is functionally involved in the response to salt stress. *OsCIPK24* and *OsCBL4* serve as the homologs of *AtSOS2* and *AtSOS3*, respectively. The OsCIPK24-OsCBL4 complex forms a functional module with OsSOS1 to confer Na^+ tolerance [7]. Beyond the SOS pathway, multiple additional genes in rice modulate salt tolerance by maintaining ion homeostasis. OsCaM1-1 positively regulates rice salt tolerance through Ca^{2+} signaling, which modulates the homeostasis of Na^+ and K^+ [8]. Notably, the expression of these ion homeostasis-related genes and their associated regulatory processes are frequently governed by transcription factors. Transcription factors act as core regulatory units in plant responses to salt stress, attributed to their extensive regulatory networks and functional diversity. Accumulating studies have highlighted their pivotal role in stress signaling cascades. OsLHY enhances salt tolerance via regulating Na^+/K^+ balance [9]. OsARF12 transcriptionally activates the expression of key ion transporter genes, including *OsSOS1* and *OsHKT1;5*, thereby improving salt tolerance in rice [10]. The transcription factor OsWRKY72 strengthens salt tolerance through SKC1-mediated Na^+ regulation [11]. OsMYB9 promotes salt tolerance by orchestrating vacuolar Na^+ sequestration [12].

Significant progress has been made in the identification of salt tolerance-related genes in rice, with a total of 207 genes identified and distributed across all 12 chromosomes, providing an important genomic resource for dissecting the regulatory networks underlying salt tolerance [13]. Among these identified genes, multiple transcription factors have been confirmed to directly participate in the regulation of salt stress, a major abiotic stressor. At the transcriptional level, several canonical transcription factor families have been validated to play key regulatory roles in plant salt stress responses, including WRKY [14], NAC [15], and bZIP [16] families. These transcription factors precisely activate or repress the expression of salt-responsive genes by recognizing and binding to specific cis-acting elements within the promoter regions of target genes. Representative cis-acting elements include

the W-box targeted by WRKY proteins [13], the NACRS bound by NAC proteins [17], and the ABRE recognized by bZIP factors [18]. Through such interactions, transcription factors integrate stress signals and modulate physiological metabolic processes such as osmolyte synthesis and reactive oxygen species scavenging, ultimately enhancing plant adaptability to saline environments.

For instance, OsWRKY53 functions as a negative regulator of salt stress. It suppresses the transcription of *OsMKK10.2* and *OsHKT1;5* by binding to their promoters, thereby modulating salt tolerance-related processes [19]. In contrast, OsWRKY28 positively regulates rice salt tolerance through direct binding and activation of *OsDREB1B*, a key salt-responsive gene [20]. Additionally, genes such as *OsbZIP72* [21], *OsMYB2* [22], *OsNAC45* [23], and Os*NAC005* [24] contribute to salt tolerance by regulating the expression of downstream stress-responsive genes. These target genes include those encoding proline synthases, catalases, and ion transporters, which are involved in critical physiological processes such as osmotic balance maintenance, oxidative damage repair, and ion homeostasis regulation. Collectively, these findings establish the central role of transcription factors in the regulatory network governing rice salt stress responses. The NAC family represents one of the largest plant-specific transcription factor families [25]. In rice, NAC proteins play important roles in root development and drought tolerance [26].

Despite the characterization of partial transcription factors, the dynamic regulatory networks of salt tolerance-related transcription factors in rice and the cooperative interaction mechanisms among their members remain to be systematically elucidated. Particularly, roots serve as the primary organ for perceiving and responding to salt stress [27], yet the regulatory rules of transcription factors in root salt stress responses lack systematic interpretation. Based on this, the present study focuses on rice seedling roots, aiming to identify the transcription factor regulatory networks involved in salt stress responses. It is expected to provide new theoretical basis for improving our understanding of the molecular mechanisms underlying rice salt tolerance.

2. Materials and Methods

Experimental materials

The indica two-line hybrid rice male sterile line ZH11 (Zhonghua 11) was used as the experimental material. Seeds were soaked in distilled water for two days to initiate germination. Upon radicle emergence, seedlings were transferred to NaCl solutions with different concentrations for salt stress treatment. The treatment duration was seven days. Four experimental groups were established: a control group (CK) treated with distilled water, a low salt group (NCL1) treated with 0.125% NaCl, a moderate salt group (NCL2) treated with 0.25% NaCl, and a high salt group (NCL3) treated with 0.5% NaCl. Each treatment included three independent biological replicates. After seven days of salt stress treatment, five uniformly growing seedlings were randomly selected from each group for phenotypic analysis. Growth parameters including primary root length, lateral root length, and shoot length were measured.

RNA Extraction, library construction, and sequencing

Frozen rice root samples (50 ~ 100 mg) preserved in liquid nitrogen were placed into a pre-chilled mortar, and additional liquid nitrogen was added to facilitate rapid grinding into a fine powder. The powdered tissue was transferred to a 1.5 mL centrifuge tube, immediately homogenized in 1 mL of TRIzol® reagent, vortexed vigorously to ensure complete mixing, and incubated at room temperature for 5 min. Subsequently, 200 μL of chloroform was added; the tube was shaken vigorously for 15 s and then incubated at room temperature for another 5 min. The mixture was centrifuged at 12,000 rpm for 15 min at 4°C. The upper aqueous phase (approximately 400 μL) was carefully pipetted into a new centrifuge tube, with strict avoidance of the intermediate protein layer. An equal volume of isopropanol (approximately 400 μL) was added, and the tube was gently inverted to mix thoroughly, followed by incubation at room temperature for 10 min to precipitate RNA. After centrifugation at 12,000 rpm for 10 min, the supernatant was discarded, and white RNA pellets were visible at the tube bottom.

RNA quality was assessed using an Agilent 2,100 Bioanalyzer (Agilent Technologies, Santa Clara, CA, USA) and verified by 1% agarose gel electrophoresis. Ribosomal RNA (rRNA) was depleted using a standard rRNA removal kit to enrich messenger RNA (mRNA). The extracted mRNA was further purified and concentrated with mRNA Capture Beads. Post bead purification, mRNA was fragmented by thermal treatment. Using these fragmented mRNA molecules as templates, the first strand of complementary DNA (cDNA) was synthesized in a reverse transcriptase reaction system. During the synthesis of the second cDNA strand, end repair and poly(A) tailing were simultaneously accomplished. Adapter ligation was then performed, and target fragments were purified and selected using Hieff NGS® DNA Selection Beads. Finally, library amplification was carried out via polymerase chain reaction (PCR). Sequencing was performed on an Illumina HiSeq 2,500 platform (Illumina, San Diego, CA, USA) following the manufacturer's protocols.

Data analysis and reference genome alignment

Raw transcriptomic sequencing data were quality controlled using fastp software [28] to generate high-quality clean reads. The QC process involved removing adapter-contaminated reads, filtering sequences with > 10% N bases, eliminating poly(A) tail artifacts, and discarding low-quality reads (defined as containing ≥ 50% bases with a Phred quality score Q ≤ 20). This stringent QC pipeline ensured the reliability of subsequent analyses. To eliminate interference from residual rRNA in the transcriptomic dataset, bowtie2 [29] was employed to efficiently identify and remove rRNA-derived sequences, retaining biologically meaningful unmapped reads for the construction of a high-quality analytical dataset. The publicly available rice reference genome Os-Nipponbare-Reference-IRGSP-1.0_Release_7 was used for alignment. Clean reads were efficiently mapped to the reference genome using HISAT2 software [30], which leverages hierarchical indexing technology to enhance alignment accuracy and speed. Based on the high-precision alignment results, Stringtie [31] was used for transcript reconstruction with the parameter setting -f 0.3. The relative expression levels of all genes in each sample were quantified using RSEM [32], which calculates expected read counts for each transcript.

Differential gene expression analysis, functional enrichment and network construction

Principal Component Analysis (PCA) was performed on the gene expression matrix using the R platform (v4.3.0) to evaluate the overall variation and reproducibility among biological replicates. For DEG analysis, raw read count data were normalized using DESeq2 software [33], a tool specifically designed for differential expression analysis of count data. Statistical testing of DEGs was conducted based on a negative binomial distribution model to calculate p-values, which were then adjusted using the Benjamini-Hochberg method to control for false positives, yielding the False Discovery Rate (FDR). DEGs were identified using the criteria of $|\log_2(\text{Fold Change})| > 1$ and FDR < 0.05. Additionally, genome-wide pathway enrichment analysis was performed using the Kyoto Encyclopedia of Genes and Genomes (KEGG) database (www.genome.jp/kegg) to systematically identify the signaling pathways and metabolic networks associated with DEGs. To further investigate the interaction patterns among DEGs, a protein-protein interaction (PPI) network was constructed based on interaction data retrieved from the STRING database (v11.5) [34] with a confidence score threshold of 0.7. Cytoscape software (v3.10.2) [35] was used for network visualization and core module mining via the MCODE plugin, thereby deciphering the regulatory mechanisms of DEGs at the protein interaction level.

Total RNA extraction and real-time PCR analysis

Total RNA was extracted from 100 mg of rice seedling root tissue using Trizol reagent (Invitrogen). According to the manufacturer's instructions, the purified RNA was reverse-transcribed into cDNA using the PrimeScript RT reagent Kit (TaKaRa, Dalian, China). The real-time quantitative PCR (RT-qPCR) reaction was performed in a total volume of 20 μL using SYBR Premix ExTaq™ (TaKaRa, Dalian, China) on an ABI StepOne Plus Real-Time PCR System. Gene expression differences were expressed as fold changes relative to the control and calculated using the $2 - \Delta\Delta CT$ method. Each measurement was conducted with three technical replicates, and the error bars represent the standard deviation (SD) of the mean fold changes from three biological replicates.

Phenotypic characterization of mutants under salt stress

To systematically characterize the salt stress-responsive traits of NAC family gene homozygous mutants (*osnac1*, *osnca10*, *osnac15*, *osnac28*) with the wild-type ZH11 as the genetic background, the present study designed the following phenotypic identification experiment. All these mutant lines were purchased from the BaiGe Gene mutant library to ensure the uniformity and reliability of the materials **(**Table 1, **Figure S1)**. Plump and uniform seeds of each material were surface-sterilized with 75% ethanol for 30 s and then disinfected with 0.1% $HgCl_2$ solution for 10 min, followed by rinsing 5 ~ 6 times with sterile water to remove residual disinfectant. The treated seeds were placed in Petri dishes lined with double layers of sterile filter paper, supplemented with an appropriate volume of sterile water to maintain moisture, and germinated in a controlled-environment chamber (temperature of 28°C; photoperiod of 12 h light/12 h dark; light intensity of 12000 lx; relative humidity of 75%).

After the seeds exhibited radicle emergence (coleorhiza protruding approximately 0.5 cm beyond the seed coat), those with consistent germination status were selected and transferred separately to Petri dishes containing H_2O (control treatment) or 0.5% NaCl solution (salt stress treatment) for a 14-day

continuous culture period. During the cultivation, an equal volume of the corresponding treatment solution was replenished daily to maintain stable concentrations. At the end of the treatment, 30 plants with uniform growth were randomly selected from each material group, and phenotypic traits including taproot length, lateral root length, and shoot length were measured. Meanwhile, 3 representative seedlings were chosen from the above-mentioned plants for phenotypic photography and documentation. All the determined data were used for subsequent statistical analysis. Through systematic phenotypic observation and quantitative analysis, this experiment provides critical phenotypic evidence for elucidating the regulatory functions of *OsNAC1*, *OsNAC10*, *OsNAC15*, and *OsNAC28* genes in rice responses to salt stress.

Table 1
Information on NAC family gene homozygous mutants

Gene name	Gene locus	Type of mutation	Germplasm accession number
OsNAC1	*LOC_Os02g36880*	Homozygous T insertion	BG110030D09
OsNAC10	*LOC_Os11g03300*	Homozygous T insertion	BG110243A08
OsNAC15	*LOC_Os07g48550*	Homozygous 5-bp insertion	BG120010H06
OsNAC28	*LOC_Os02g34970*	Homozygous T insertion	BG110009E10

3. Results

Phenotypic characterization of rice seedling roots under salt stress

Salt stress exerted a significant inhibitory effect on the morphological development of rice seedlings, and this inhibitory effect intensified with increasing NaCl concentration. Results showed that seedlings in the CK (H_2O) group displayed well developed root systems and vigorous shoot growth (Fig. 1A). In contrast, seedlings exposed to NCL1 (0.125% NaCl), NCL2 (0.25% NaCl), and NCL3 (0.5% NaCl) treatments displayed clear growth retardation, characterized by dwarfism and pronounced suppression of both root (primary and lateral) and shoot development. Notably, the inhibitory effects were dose-dependent, with NCL3 exerting a stronger suppression than NCL2 and NCL1. Quantitative measurements (Fig. 1B) further substained these phenotypic differences. The primary root length reached a maximum of 11.8 cm in the control group. Following NCL1 and NCL2 treatments, primary root length decreased significantly, with no statistically difference observed between these two treatments. Under NCL3 treatment, primary root length was further reduced to 2.70 cm, showing a significant difference compared with both NCL1 and NCL2. Similarly, the suppression of lateral root formation and shoot elongation became more prounced with increasing NaCl concentration. Overall, salt stress significantly restricted the elongation of primary roots, lateral roots, and shoots in rice seedlings, with the degree of inhibition positively correlated NaCl concentration. These results clearly delineate the salt stress induced growth responses of this rice genotype and provide a robust phenotypic basis for subsequent correlation analysis.

Data Quality Control

To ensure the reliability of downstream analyses and eliminate potential interference from low quality reads, the raw sequencing data were subjected to rigrous quality control filtering. The quality control (QC) results for the transcriptomic data were obtained from nine ZH11 rice samples **(**Table 2**).** The number pf clean reads generated form each sample was high across all groups. The control group (CK) produced 43,243,773 clean reads, corresponding to more than 4.3×10^7 base pairs (bp). In the salt treatment groups, the clean read counts were 49,870,493 for NCL1, 48,406,191 for NCL2, and 47,985,791 for NCL3, all exceeding 4.7×10^7 bp indicating sufficient sequencing depth for transcriptome analysis. Evaluation of sequencing base quality further demonstrated the high reliability of the dataset. The proportion of Q20 bases (Phred quality score ≥ 20) exceeded 98.3% across all samples, specifically 98.74% in CK, 98.63% in NCL1, 98.36% in NCL2, and 98.37% in NCL3. Similarly, the proportion of Q30 bases (Phred quality score ≥ 30) remained above 95.7% across all samples, with values of 96.84% in CK, 96.45% in NCL1, 95.73% in NCL2, and 95.83% in NCL3, confirming the high base calling accuracy of the sequencing data. Genome alignment analysis showed differences in mapping efficiency among treatments. In the CK group, the total mapping rate and unique mapping rate were 37.06% and 36.21%, respectively. For NCL1, these values increased slightly to 39.28% and 38.38. The NCL2 group exhibited the highest mapping efficiency, with a total mapping rate of 67.80% and amunique mapping rate of 66.16%. In the NCL3 group, the total and unique mapping rates were 42.24% and 41.27%, respectively. Additional quality control indicators further confirmed high of the sequencing dataset. The percentage of high-quality reads exceeded 99% in all samples. Adapter contamination was minimal (< 0.1%), the proportion of low quality reads remained below 0.03%, the percentage of reads containing ambiguous N bases ranged from 0.01% to 0.06%. Moreover, no poly(A) artifact reads were detected. Collectively, these quality control metrics demonstrates that the sequencing data are of high quality and meet the stringent requirements for subsequent transcriptomic analyses.

Table 2
Quality statistical analysis of raw sequencing data

Sample	Raw data	Clean Data	≥ Q20(%)	≥ Q30(%)	Total Mapped(%)	Unique Mapped(%)
CK	43,275,807	43,243,773	6,377,082,790 (98.74%)	6,254,517,192 (96.84%)	16,002,536 (37.06%)	15,636,570 (36.21%)
NCL1	49,921,861	49,870,493	7,307,662,533 (98.63%)	7,142,634,623 (96.45%)	19,548,566 (39.28%)	19,102,171 (38.38%)
NCL2	48,472,627	48,406,191	7,075,855,425 (98.36%)	6,886,617,516 (95.73%)	32,750,575 (67.80%)	31,956,882 (66.16%)
NCL3	48,042,298	47,985,791	7,016,035,857 (98.37%)	6,834,873,942 (95.83%)	20,215,178 (42.24%)	19,754,634 (41.27%)

Transcriptomic profiling and gene expression analysis under salt stress

Total RNA was extracted from the samples, and ribosomal RNA (rRNA) was removed to enrich messenger RNA (mRNA). The enriched mRNA was subsequently reverse-transcribed into double-stranded cDNA, followed by library construction through end repair, adapter ligation and PCR amplification **(**Fig. 2A**)**. The distribution of gene expression levels measured as FPKM values, showed that majority of genes were moderately expressed, while the number of highly expressed genes were relatively few. Principal component analysis (PCA) results indicated that the first principal component (PC1) explained 31.77% of the total variance. Samples subjected to different NaCl concentrations formed distinct clusters, with strong grouping within treatments and clear separation between treatments, indicating reliable discrimination of transcriptomic differences under salt stress **(**Fig. 2C**)**. The violin plot further demonstrated that gene expression values were predominantly distributed within a moderate range, with only small proportion of highly expressed genes **(**Fig. 2D**)**. This distribution exhibited a typical right-skewed pattern. In addition, the expression profiles displayed a unimodal and approximately symmetrical distribution, suggesting good reproducibility among samples. Consistently, correlation analysis showed that samples within the same treatment group had correlation coeffecients approaching 1.00, while correlations between the control group (CK) and salt treated groups (NCL1, NCL2, NCL3) progressively decreased. These results indicate that transcriptomic variation increased with rising salt concentration, with NCL3 showing the strongest effect and NCL1 the weakest **(**Fig. 2E**)**.

To investigate the chromosomal distribution of gene expression, a total of 30,910 genes with non-zero expression levels **(Table S1)** were mapped to the 12 rice chromosomes based on their expression abundance, generating a genomewide expression profile (Fig. 2F). The results revealed a consistent positional pattern, in which genes located at the distal ends of chromosome arms exhibited relatively higher expression levels, whereas those near centromeric regions showed lower expression. K-means clustering further classified these genes into distinct expression profiles, revealing substantial differences in cluster size and expression patterns **(Table S2)**. For instance, Profile 0 contained 1,022 genes, while Profile 1 contained only 42 genes. Some gene clusters displayed dynamic and fluctuating expression patterns, whereas others exhibited relatively uniform expression trends, reflecting diverse transcriptional responses under salt stress (Fig. 2G, **Figure S2**). Analysis of specifically expressed genes showed that the total number of expressed genes in CK, NCL1, NCL2, and NCL3 groups was 26,569, 26,613, 28,419, and 26,483, respectively **(**Fig. 2H, **Table S3)**. The Venn diagram revealed that the 23,887 genes were commonly expressed across all groups, whereas, 611, 533, 1,318, and 698 genes were uniquely expressed in CK, NCL1, NCL2, and NCL3 respectively **(**Fig. 2I, **Table S4)**. The results highlight the gene expression patterns induced by varying salt concentrations. Furthermore, the expression distribution histogram showed that gene expression levels were predominantly concentrated in the low expression range, consistent with the patterns observed in the violin plots (Fig. 2J).

Functional enrichment analysis revealed the key biological pathways in rice young roots under NaCl stress

Following the removal of duplicate genes, a total of 7,687 significantly differentially expressed genes (DEGs) were identified in rice young root samples **(Table S5)** and further characterized based on their expression profiles. Statistical analysis of these DEGs **(**Fig. 3A, **Figure S3)** reflected the extent of transcriptomic perturbation under different salt concentrations. Between the control (CK) and low-concentration NaCl treatment (NCL1), 1,785 upregulated and 394 downregulated DEGs were detected, indicating that low-concentration salt stress exerts a relatively mild regulatory impact on gene expression. In contrast, the comparison between CK and the high concentration treatment revealed a substantial increase in DEGs, including 2,218 upregulated and 2,785 downregulated genes. Additionally, 3,301 downregulated DEGs were identified between the NCL2 and NCL3 groups **(Table S6)**, further demonstrating that higher salt concentrations induce stronger transcriptional reprogramming in rice young roots. The chromosomal distribution of DEGs was visualized using a Circos plot (Fig. 3B), which mapped 3,963 DEGs **(Table S7)** across the 12 rice chromosomes. This analysis also revealed the overlap of highly expressed genes among treatment. A substantial overlap was observed between CK and NCL1, whereas minimal overlap was detected between NCL2 and CK, indicating greater ranscriptomic divergence under higher salt stress. Venn diagram analysis **(**Fig. 3C**)** further clarified the overlap of DEGs among the three comparisons (CK vs NCL1, CK vs NCL2 and CK vs NCL3). A total of 299 common DEGs were identified, representing a core set of genes involved in the salt stress response. In addition, 167, 770, and 3,580 DEGs were uniquely identified in CK vs NCL1, CK vs NCL2, and CK vs NCL3 comparisons, respectively (**Table S8**), providing candidate genes associated with responses to different salt intensities. Expression heatmap analysis (Fig. 3D, Fig. 3E), showed that most of these core DEGs exhibited increased expression under moderate and high salt treatments. This consistent expression pattern suggests their involvement in early salt stress perception and response in rice young roots.

KEGG pathway enrichment analysis **(**Fig. 3F**)** further revealed distinct metabolic responses under different salt concentrations. Under low-salt conditions, DEGs were enriched in pathways such as photosynthesis, carbon fixation in the Calvin cycle and nitrogen metabolism, indicating maintenance of basic metabolic processes. Under moderate-salt stress, enrichment was observed in pathways including indole alkaloid biosynthesis, ABC transporters and arginine and proline metabolism, reflecting enhanced ion transport and osmotic adjustment. Under high-salt stress, DEGs were enriched in a broader range of pathways, including glutathione metabolism, starch and sucrose metabolism and alpha-linolenic acid metabolism, suggesting activation of antioxidant systems, osmotic adjustment, and stress related metabolic pathways. Notably, secondary metabolism related pathways were enriched across all treatments, indicating their fundamental role in the response of rice young roots to salt stress..

WGCNA reveals coexpression modules, key transcription factors, and functional pathways in rice under salt stress

Weighted Gene Co-expression Network Analysis (WGCNA) was performed to identify gene modules associated with salt stress in rice ZH11. The module–trait relationship heatmap (Fig. 4A) revealed the correlation between gene modules and different salt treatments (CK, NCL1, NCL2, and NCL3). Notably, modules such as MEred exhibited strong positive correlations with high salt treatment (NCL3), indicating

their potential involvement in salt stress responses in rice young roots. Genes were clustered into distinct co-expression modules using a dynamic tree-cutting method, and an appropriate soft-threshold was selected to ensure a scale-free network topology, thereby providing a reliable framework for downstream analysis **(**Fig. 4B**)**. A total of 5,591 key module genes were identified via WGCNA **(Table S9)**. The expression heatmap of these key genes showed clear variation in expression patterns across different salt concentrations, with pronounced changes under high-salt treatment (NCL3), consistent with the module-trait association results **(**Fig. 4C**)**. Functional enrichment analysis further characterized the biological roles of core module genes. KEGG enrichment results **(Figure S4A)** showed significant enrichment in pathways such as amino acid biosynthesis, carbohydrate metabolism, and glutathione metabolism, which are associated osmotic adjustment, energy supply, and oxidative stress mitigation. Furthermore, pathway enrichment analysis **(Figure S4B)** highlighted the involvement of signaling pathways including plant hormone signal transduction and the MAPK signaling pathway, indicating coordinated regulation of multiple pathways under the salt stress. Co-expression network analysis **(**Fig. 4D**)** identified 89 key hub genes from the core modules. Among these, several transcription factors from major families such as (bHLH, NAC, WRKY, and bZIP), such as *OsbHLH035*, *OsNAC10*, and *OsbZIP46*, occupied central positions within the network, supporting their role in the salt stress responses. Further analysis of transcription factor networks (Fig. 4E) identified 99 core transcription factors, with WRKY, NAC, and bHLH families being predominant. A Venn diagram **(**Fig. 4F**)** comparing transcription factors identified by WGCNA and those among the DEGs revealed ten overlapping genes. The expression heatmap of these ten genes **(**Fig. 4G**)** showed consistently highly expression under high salt concentration treatment, indicating their potential roles as key regulators in the salt stress response. Overall, the integration of WGCNA, functional enrichment, and transcription factor network analysis identified core co-expression modules, key regulatory genes, and major biological pathways associated with salt stress responses in rice young roots, providing a basis for further functional studies..

RT-qPCR alidvation of salt responsive transcription factors

To validate the reliability of transcriptome data, ten core transcription factors were selected for RT-qPCR validation, including *OsbHLH035*, *OsERF113*, *OsMYBS3*, five NAC family members (*OsNAC1*, *OsNAC10*, *OsNAC15*, *OsNAC28*, *OsNAC073*), and two WRKY family members *(OsWRKY23*, *OsWRKY74*). The RT-qPCR results **(**Fig. 5**)** showed that eight transcription factors, namely *OsbHLH035*, *OsERF113*, *OsNAC1*, *OsNAC10*, *OsNAC15*, *OsNAC28*, *OsNAC073*, and *OsWRKY23*, exhibited a a gradual increase in expression levels with increasing NaCl concentration. Among these, *OsERF113* and *OsNAC28* displayed the most pronounced upregulation. In contrast, *OsMYBS3* and *OsWRKY74* showed distinct expression patterns. *OsMYBS3* reached peak expression at the NCL2 treatment, whereas *OsWRKY74* was significantly upregulated only under the NCL3 treatment. Further analysis of tissue specific expression patterns **(Figure S5)** indicated that most of these transcription factors, including *OsbHLH035*, *OsERF13*, *OsWRKY23*, *OsNAC1*, *OsNAC10*, *OsNAC15*, *OsNAC28*, are specifically expressed in roots. Overall, the RT-qPCR results were consistent with the transcriptome data, confirming the reliability of the RNA-seq analysis. In addition, these results highlight the prominent role of NAC family transcription factors in the

response of rice to salt stress and demonstrate distinct expression dynamics among different transcription factor members.

Phenotypic characterization of NAC mutants under salt stress

To investigate the functions of NAC family genes, homozygous mutant lines, including *osnac1* (with a T base insertion), *osnac10* (with a T base insertion), *osnac15* (with a 5-bp insertion), and *osnac28* (with a T base insertion), were generated, with wild-type ZH11 used as the control. All materials were subjected to 14 day treatments under H_2O (control) and 0.5% NaCl (salt stress), followed by phenotypic evaluation **(**Fig. 6**)**. Under H_2O treatment, ZH11 seedlings exhibited optimal growth, characterized by greater plant height longer primary and lateral roots with a dense root system. In contrast, *osnac1* seedlings showed the most severe growth inhibition, with significantly reduced plant height, shortened roots, and sparse lateral root development. The *osnac10* and *osnac15* mutants displayed intermediate phenotypes, with growth parameters lower than ZH11 but clearly improved compared with *osnac1*. The *osnac28* mutant showed no obvious phenotypic differences from ZH11. Quantitative analysis of primary root length, lateral root length, and shoot length (Fig. 6A) confirmed that all three traits were significantly reduced in *osnac1*, moderately reduced in *osnac10* and *osnac15*, and unchanged in *osnac28* compared with ZH11.

Following 14 days of 0.5% NaCl stress treatment, wild-type ZH11 had the longest primary and lateral roots among all, but no significant advantage in shoot length. The *osnac1*, *osnac10*, and *osnac15* mutants exhibited shorter roots compared with ZH11, indicating enhanced sensitivity to salt stress. However, differences in shoot length between these mutants and ZH11 were less pronounced. The *osnac28* mutant showed slightly shorter roots and comparable shoot length relative to ZH11, with no significant phenotypic differences **(**Fig. 6B**)**, consistent with its behavior under control (H_2O) conditions.

These results demonstrate functional differentiation among NAC family genes in regulating rice seedling growth and salt stress responses. Under normal conditions, loss of *OsNAC1*, *OsNAC10*, *OsNAC15* significantly impaired growth, whereas *OsNAC28* had minimal effect. Under salt stress, root growth inhibition was more pronounced in *osnac1*, *osnac10*, and *osnac15*, suggesting their involvement in regulating root development under stress conditions. Consistently, the single-cell transcriptome atlas of rice roots (**Figure S6**) showed that these genes are highly expressed in root tissues, supporting their functional roles in root growth and providing phenotypic evidence for further investigation of their molecular mechanisms in salt stress adaptation.

4. Discussion

Salt stress severely restricts rice growth, particularly at the seedling stage, where plants exhibit the highest sensitivity to saline conditions. The root system serves as the primary site for salt perception and response, thereby playing a decisive role in seedling establishment and final yield. In this context, elucidating the transcriptional regulatory networks underlying salt stress responses in rice roots is essential for both fundamental research and breeding applications. In the present study, the two line male sterile line ZH11 was subjected to gradient NaCl treatments combined with RNA-seq analysis to

systematically characterize differentially expressed genes (DEGs) and their associated biological pathways.

Compared with previous studies that typically employed a single NaCl concentration and focused on later developmental stages [36], his study utilized gradient salt treatments at the early seedling stage, enabling a more refined dissection of transcriptional responses under varying stress intensities. While earlier work identified 12,898 salt-responsive DEGs at the population level [37], our approach integrated DEG analysis with weighted gene co-expression network analysis (WGCNA), thereby improving the precision of key gene identification and enhancing the reliability of candidate regulators for downstream functional studies.

Phenotypic observations demonstrated a clear concentration dependent inhibition of seedling growth under salt stress, particularly affecting primary root, lateral root, and shoot development. Transcriptomic analysis identified 299 common DEGs across treatments, representing a core regulatory module for salt stress responses, whereas treatment-specific DEGs reflected adaptive mechanisms unique to different salt concentrations. Functional enrichment analysis revealed that low salt conditions primarily activated pathways associated with osmotic adjustment and ion transport, whereas high salt stress triggered pathways related to secondary metabolism and glutathione metabolism, which are essential for stress adaptation. Notably, secondary metabolic pathways were consistently enriched across all treatments, underscoring their central role in salt tolerance.

Weighted gene co-expression network analysis further identified key co-expression modules strongly associated with high salt stress. Genes within these core modules were enriched in pathways related to amino acid metabolism, sugar metabolism, glutathione metabolism as well as hormone and mitogen-activated protein kinase signaling pathways. These pathways collectively maintain physiological homeostasis in young roots under salt stress. Among the 88 key hub genes identified through co-expression network analysis, members of transcription factor families including bHLH, NAC, WRKY and bZIP occupied central positions in the regulatory network. Ten transcription factors were found in both core modules and the set of DEGs. These transcription factors included *OsbHLH035*, *OsNAC028*, *OsNAC15*, *OsNAC10*, *OsNAC1*, *OsERF113*, *OsNAC073*, *OsWRKY74*, *OsMYBS3* and *OsWRKY23*. Among them, *OsNAC1*, *OsNAC10* and *OsNAC15* were identified as key candidate genes mediating salt stress responses. Combined with mutant phenotype validation results showing that loss of function of these genes regulated root growth under salt stress, our findings further confirmed that *OsNAC1*, *OsNAC10* and *OsNAC15* are key regulators of salt stress responses in the tested rice material.

Previous studies have shown that *OsNAC1* is involved in drought tolerance [38], and our findings extend its functional role to salt stress, suggesting a broader involvement in abiotic stress crosstalk. similarly, *OsNAC15* has been reported in previous studies to regulate salt tolerance in rice [39], which is consistent with our results and further supports its conserved role. Additionally, among the 151 annotated NAC family genes in the rice genome, *OsNAC5* [40], *OsNAC6* [41], *OsNAC9* [42], *OsNAC10* [43] and *OsNAC120*

[44] have all been confirmed to be closely related to salt tolerance. These genes together form a key NAC family regulatory unit in the rice salt stress response pathway.

In summary, this study provides a systematic analysis of transcriptional regulation, co-expression networks, and functional pathways underlying salt stress responses in rice seedling roots. The integration of phenotypic, transcriptomic, and network analyses enabled the identification of key regulatory genes and pathways, thereby advancing our understanding of salt adaptation mechanisms. These findings offer valuable candidate genes and a theoretical framework for future functional validation and the development of salt tolerant rice varieties.

Aabbreviation

All abbreviations used in the manuscript are defined at their first occurrence. The full list of abbreviations is as follows:

Short form	Full form
CK	ZH11; Zhonghua 11
NCL1	0.125% NaCl treatment group
NCL2	0.25% NaCl treatment group
NCL3	0.5% NaCl treatment group
RNA-seq	RNA sequencing
DEGs	Differentially Expressed Genes
GWAS	Genome-Wide Association Study
QTLs	Quantitative Trait Loci
WGCNA	Weighted Gene Co-expression Network Analysis
PPI	Protein-Protein Interaction
KEGG	Kyoto Encyclopedia of Genes and Genomes
FPKM	Fragments Per Kilobase of transcript per Million mapped reads
RT-qPCR	Reverse Transcription Quantitative Polymerase Chain Reaction

Declarations

Ethics approval and consent to participate

This study did not involve human participants, animal experiments, or collection of protected species. All plant material collection and experiments complied with relevant institutional, national, and international

guidelines and legislation and and written informed consent was obtained from all participants.

Consent for publication

Not applicable.

Competing interests

The authors declare that they have no competing interests.

Funding

This work was supported by the Key Areas Research Projects of Guangdong Province (2022B0202060002), The earmarked fund for Modern Agro-industry Technology Research System (CARS-01), Guangdong Key Laboratory of Rice Science and Technology(2023B1212060042).

Author Contribution

Y.Z. and T.C. wrote the manuscript draft, data analysis, H.L. provided the realtime PCR validation, D.L. provided the raw sequence data analysis, Umer and Sunil supported the language editing improvement, W.L. design this experiment, F.W. revised the draft, W.L., F.W., and X .H. obtained the fund.

Acknowledgements

The authors gratefully acknowledge the financial support provided by the scientific research project. We thank all members of our laboratory for their assistance and valuable suggestions during the experiment. Meanwhile, we sincerely appreciate the editors and anonymous reviewers for their constructive comments to improve this manuscript.

Data Availability

The raw sequence data have been deposited in the Science Data Bank (https://www.scidb.cn). The open-access raw bulk RNA-seq data of rice seedling roots under salt stress are available at: https://www.scidb.cn/s/ayyqmm.

References

1. Yang Y, Guo Y. Elucidating the molecular mechanisms mediating plant salt-stress responses. New Phytol, 2018, 217(2):523–539. https://doi.10.1111/nph.14920.

2. Munns R, Tester M. Mechanisms of salinity tolerance. Annu Rev Plant Biol. 2008, 59:651 – 81. https://doi.10.1146/annurev.arplant.59.032607.092911.
3. Ismail AM, Horie T. Genomics, physiology, and molecular breeding approaches for improving salt tolerance. Annu Rev Plant Biol. 2017, 68:405–434. https://doi.10.1146/annurev-arplant-042916-040936.
4. Chunthaburee S, Dongsansuk A, Sanitchon J, Pattanagul W, Theerakulpisut P. Physiological and biochemical parameters for evaluation and clustering of rice cultivars differing in salt tolerance at seedling stage. Saudi J Biol Sci. 2016, 23(4):467 – 77. https://doi.10.1016/j.sjbs.2015.05.013.
5. Shi H, Lee BH, Wu SJ, Zhu JK. Overexpression of a plasma membrane Na^+/H^+ antiporter gene improves salt tolerance in Arabidopsis thaliana. Nat Biotechnol. 2003, 21(1):81 – 5. https://doi.10.1038/nbt766.
6. Ma L, Han R, Yang Y, Liu X, Li H, Zhao X, Li J, Fu H, Huo Y, Sun L, Yan Y, Zhang H, Li Z, Tian F, Li J, Guo Y. Phytochromes enhance SOS2-mediated PIF1 and PIF3 phosphorylation and degradation to promote Arabidopsis salt tolerance. Plant Cell. 2023, 35(8):2997–3020. https://doi.10.1093/plcell/koad117.
7. Martínez-Atienza J, Jiang X, Garciadeblas B, Mendoza I, Zhu JK, Pardo JM, Quintero FJ. Conservation of the salt overly sensitive pathway in rice. Plant Physiol. 2007, 143(2):1001-12. https://doi.10.1104/pp.106.092635.
8. Wei S, Chen M, Wang F, Tu Y, Xu Y, Fu L, Zeng F, Zhang G, Wu D, Shen Q. OsCaM1-1 is responsible for salt tolerance by regulating Na^+/K^+ homoeostasis in rice. Plant Cell Environ. 2025, 48(2):1393–1408. https://doi.10.1111/pce.15212.
9. Li C, He YQ, Yu J, Kong JR, Ruan CC, Yang ZK, Zhuang JJ, Wang YX, Xu JH. The rice late elongated hypocotyl enhances salt tolerance by regulating Na^+/K^+ homeostasis and ABA signalling. Plant Cell Environ. 2024, 47(5):1625–1639. https://doi.10.1111/pce.14835.
10. Cheng Y, Du K, Li G, Wang R, Tian H, Liu Y, Li F, Zhao Q, Peng T, Zhang J, Yafan Zhao. The rice auxin response factor OsARF12 coordinates ROS scavenging, photosynthetic protection, and Na^+/K^+ homeostasis under salt stress. The Crop Journal. 2025,13(6):1706–1717. https://doi.10.1016/j.cj.2025.10.004.
11. Li C, Guan J, Liang WH, Yao S, He L, Wei XD, Zhao L, Zhou LH, Zhao CF, Zhao QY, Zhu Z, Huang SD, Wang CL, Zhang YD, Lu K, Chen T. OsWRKY72 enhances salt tolerance in rice via SKC1-mediated Na^+ regulation. Plant Stress. 2025;17:100962. https://doi.org/10.1016/j.stress.2025.100962.
12. Kim B, Cho S-H, Shim Y, Yoon H, Paek N-C, Kang K. Rice OsMYB9 enhances salt stress tolerance by regulating the vacuolar Na^+/H^+ antiporter. The Crop Journal, 2025, 13: 1718–1730. https://doi.10.1016/j.cj.2025.08.002.
13. Liu CT, Mao BG, Yuan DY, Chu CC, Duan MJ. Salt tolerance in rice: physiological responses and molecular mechanisms. Crop J. 2022;10(1):13–25. https://doi.org/10.1016/j.cj.2021.02.010.
14. Li TT, Li B, Wang YY, Xu JY, Li WL, Chen ZH, Mou WS, Xue DW. WRKY transcription factors in rice: key regulators orchestrating development and stress resilience. Plant Cell Environ. 2025, 48(11):8388–

8406. https://doi.10.1111/pce.70124.

15. Xiong H, He H, Chang Y, Miao B, Liu Z, Wang Q, Dong F, Xiong L. Multiple roles of NAC transcription factors in plant development and stress responses. J Integr Plant Biol. 2025, 67(3):510–538. https://doi.10.1111/jipb.13854.
16. Xu Z, Yang Y, Zhang F, Li H, Ma H, Wu W, Ding Y. OsbZIP27 coordinates with OsHUB1 and OsHUB2 to modulate drought tolerance in rice. J Genet Genomics. 2025, 52(2):168–178. https://doi.10.1016/j.jgg.2024.11.016.
17. Tran LS, Nakashima K, Sakuma Y, Simpson SD, Fujita Y, Maruyama K, Fujita M, Seki M, Shinozaki K, Yamaguchi-Shinozaki K. Isolation and functional analysis of Arabidopsis stress-inducible NAC transcription factors that bind to a drought-responsive cis-element in the early responsive to dehydration stress 1 promoter. Plant Cell. 2004, 16(9):2481-98. https://doi.10.1105/tpc.104.022699.
18. Fujita Y, Yoshida T, Yamaguchi-Shinozaki K. Pivotal role of the AREB/ABF-SnRK2 pathway in ABRE-mediated transcription in response to osmotic stress in plants. Physiol Plant. 2013, 147(1):15–27. https://doi.10.1111/j.1399-3054.
19. Yu J, Zhu C, Xuan W, An H, Tian Y, Wang B, Chi W, Chen G, Ge Y, Li J, Dai Z, Liu Y, Sun Z, Xu D, Wang C, Wan J. Genome-wide association studies identify OsWRKY53 as a key regulator of salt tolerance in rice. Nat Commun. 2023, 14(1):3550. https://doi.10.1038/s41467-023-39167-0.
20. Zhang M, Zhao R, Wang H, Ren S, Shi L, Huang S, Wei Z, Guo B, Jin J, Zhong Y, Chen M, Jiang W, Wu T, Du X. OsWRKY28 positively regulates salinity tolerance by directly activating *OsDREB1B* expression in rice. Plant Cell Rep. 2023, 42(2):223–234. https://doi.10.1007/s00299-022-02950-2.
21. Liu X, Guo X, Li T, Wang X, Guan Y, Wang D, Wang Y, Ji X, Gao Q, Ji J. OsGSK1 interacts with OsbZIP72 to regulate salt response in rice. Plant J. 2025, 121(6):e70112. https://doi.10.1111/tpj.70112.
22. Nie S, Huang W, He C, Wu B, Duan H, Ruan J, Zhao Q, Fang Z. Transcription factor OsMYB2 triggers amino acid transporter *OsANT1* expression to regulate rice growth and salt tolerance. Plant Physiol. 2025, 197(2):kiae559. https://doi.10.1093/plphys/kiae559.
23. Zhang X, Long Y, Huang J, Xia J. OsNAC45 is involved in ABA response and salt tolerance in rice. Rice (N Y). 2020, 13(1):79. https://doi.10.1186/s12284-020-00440-1.
24. Kim Y, Kim B, Kang J, Bae SI, Yoon H, Shin HJ, Lee JY, Paek NC, Kang K. ONAC005 enhances salt stress tolerance by promoting suberin deposition in root endodermis. Plant J. 2025, 123(5):e70469. https://doi.10.1111/tpj.70469.
25. Olsen AN, Ernst HA, Leggio LL, Skriver K. NAC transcription factors: structurally distinct, functionally diverse. Trends Plant Sci. 2005, 10(2):79–87. https://doi.10.1016/j.tplants.2004.12.010.
26. Agnieszka JMirosławK, ,Iwona S. Gene expression regulation in roots under drought. J Exp Bot. 2016, 67(4):1003-14. https://doi.10.1093/jxb/erv512.
27. Galvan-Ampudia CS, Julkowska MM, Darwish E, Gandullo J, Korver RA, Brunoud G, Haring MA, Munnik T, Vernoux T, Testerink C. Halotropism is a response of plant roots to avoid a saline environment. Curr Biol. 2013, 23(20):2044-50. https://doi.10.1016/j.cub.2013.08.042.

28. Chen S, Zhou Y, Chen Y, Gu J. fastp: an ultra-fast all-in-one FASTQ preprocessor. Bioinformatics. 2018, 34(17):i884-i890. https://doi.10.1093/bioinformatics/bty560.
29. Langmead B, Salzberg SL. Fast gapped-read alignment with Bowtie 2. Nat Methods. 2012, 9(4):357-9. https://doi.10.1038/nmeth.1923.
30. Kim D, Langmead B, Salzberg SL. HISAT: a fast spliced aligner with low memory requirements. Nat Methods. 2015, 12(4):357 – 60. https://doi.10.1038/nmeth.3317.
31. Pertea M, Pertea GM, Antonescu CM, Chang TC, Mendell JT, Salzberg SL. StringTie enables improved reconstruction of a transcriptome from RNA-seq reads. Nat Biotechnol. 2015, 33(3):290-5. https://doi.10.1038/nbt.3122.
32. Li B, Dewey CN. RSEM: accurate transcript quantification from RNA-Seq data with or without a reference genome. BMC Bioinformatics. 2011, 12:323. https://doi.10.1186/1471-2105-12-323.
33. Love MI, Huber W, Anders S. Moderated estimation of fold change and dispersion for RNA-seq data with DESeq2. Genome Biol. 2014, 15(12):550. https://doi.10.1186/s13059-014-0550-8.
34. Szklarczyk D, Franceschini A, Wyder S, Forslund K, Heller D, Huerta-Cepas J, Simonovic M, Roth A, Santos A, Tsafou KP, Kuhn M, Bork P, Jensen LJ, von Mering C. STRING v10: protein-protein interaction networks, integrated over the tree of life. Nucleic Acids Res. 2015, 43(Database issue):D447-52. https://doi.10.1093/nar/gku1003.
35. Shannon P, Markiel A, Ozier O, Baliga NS, Wang JT, Ramage D, Amin N, Schwikowski B, Ideker T. Cytoscape: a software environment for integrated models of biomolecular interaction networks. Genome Res. 2003, 13(11):2498 – 504. https://doi.10.1101/gr.1239303.
36. Kong W, Sun T, Zhang C, Deng X, Li Y. Comparative transcriptome analysis reveals the mechanisms underlying differences in salt tolerance between indica and japonica rice at seedling stage. Front Plant Sci. 2021, 12:725436. https://doi.10.3389/fpls.2021.725436.
37. Wei H, Wang X, Zhang Z, Yang L, Zhang Q, Li Y, He H, Chen D, Zhang B, Zheng C, Leng Y, Cao X, Cui Y, Shi C, Liu Y, Lv Y, Ma J, He W, Liu X, Xu Q, Yuan Q, Yu X, Wang T, Qian H, Li X, Zhang B, Zhang H, Chen W, Guo M, Dai X, Wang Y, Zheng X, Guo L, Xie X, Qian Q, Shang L. Uncovering key salt-tolerant regulators through a combined eQTL and GWAS analysis using the super pan-genome in rice. Natl Sci Rev. 2024, 11(4):nwae043. https://doi.10.1093/nsr/nwae043.
38. Alafari HA, Freeg H, Abdelrahman M, Attia KA, Jalal AS, El-Banna A, Aboshosha A, Fiaz S. Integrated analysis of yield response and early stage biochemical, molecular, and gene expression profiles of pre-breeding rice lines under water deficit stress. Sci Rep. 2024, 14(1):17855. https://doi.10.1038/s41598-024-60863-4.
39. Ao CW, Xiang GJ, Wu YF, Wen Y, Zhu ZL, Sheng F, Du X. OsNAC15 regulates drought and salt tolerance in rice. Physiol Mol Biol Plants. 2024, 30(11):1909–1919. https://doi.10.1007/s12298-024-01529-3.
40. Jeong JS, Kim YS, Redillas MC, Jang G, Jung H, Bang SW, Choi YD, Ha SH, Reuzeau C, Kim JK. *OsNAC5* overexpression enlarges root diameter in rice plants leading to enhanced drought tolerance

and increased grain yield in the field. Plant Biotechnol J. 2013, 11(1):101 – 14. https://doi.10.1111/pbi.12011.

41. Lee DK, Chung PJ, Jeong JS, Jang G, Bang SW, Jung H, Kim YS, Ha SH, Choi YD, Kim JK. The rice OsNAC6 transcription factor orchestrates multiple molecular mechanisms involving root structural adaptions and nicotianamine biosynthesis for drought tolerance. Plant Biotechnol J. 2017, 15(6):754–764. https://doi.10.1111/pbi.12673.
42. Redillas MC, Jeong JS, Kim YS, Jung H, Bang SW, Choi YD, Ha SH, Reuzeau C, Kim JK. The overexpression of *OsNAC9* alters the root architecture of rice plants enhancing drought resistance and grain yield under field conditions. Plant Biotechnol J. 2012, 10(7):792–805. https://doi.10.1111/j.1467-7652.
43. Chung PJ, Jung H, Choi YD, Kim JK. Genome-wide analyses of direct target genes of four rice NAC-domain transcription factors involved in drought tolerance. BMC Genomics. 2018, 19(1):40. https://doi.10.1186/s12864-017-4367-1.
44. Xie Z, Jin L, Sun Y, Zhan C, Tang S, Qin T, Liu N, Huang J. OsNAC120 balances plant growth and drought tolerance by integrating GA and ABA signaling in rice. Plant Commun. 2024, 5(3):100782. https://doi.10.1016/j.xplc.2023.100782.

Figures

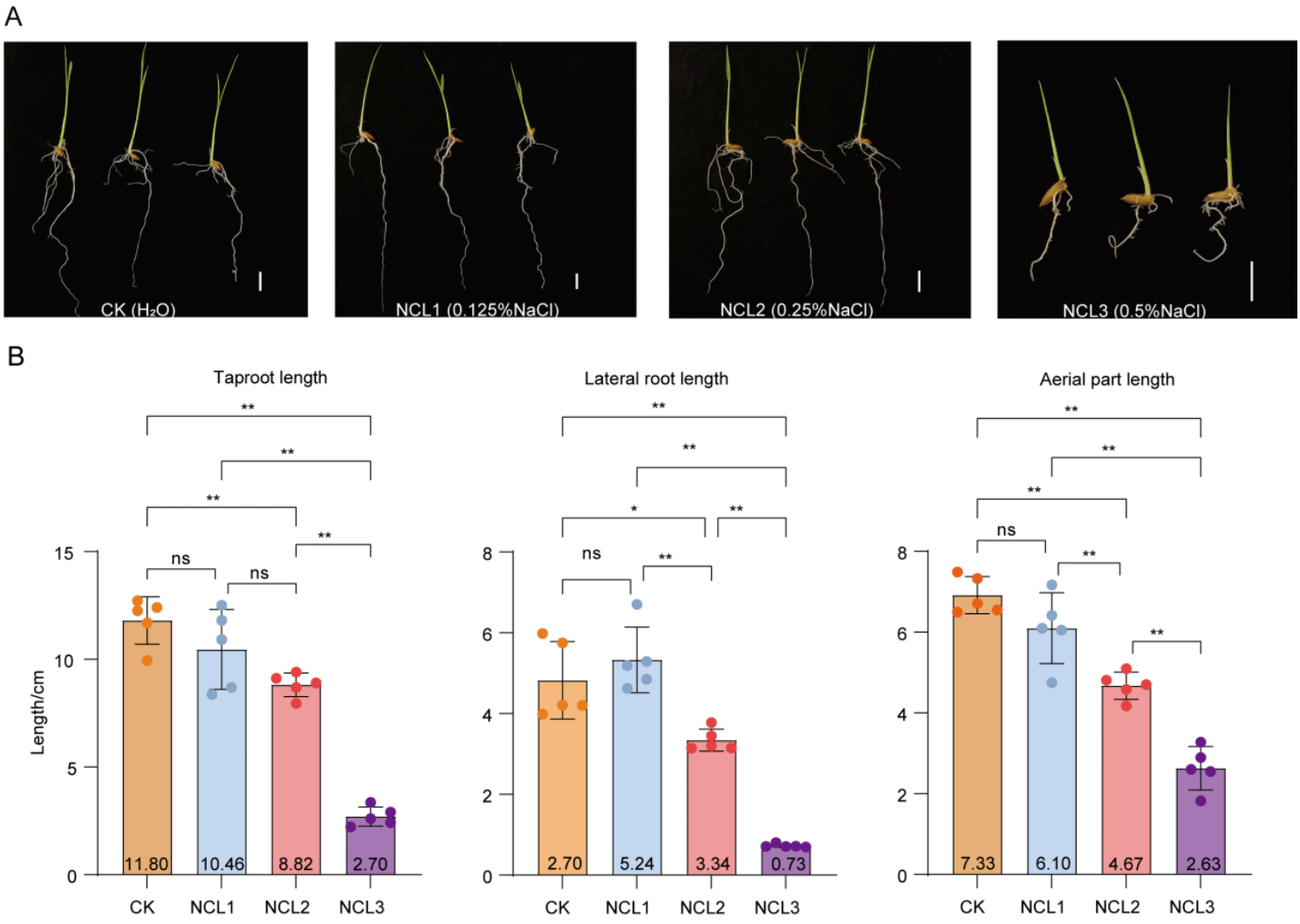


Figure 1

Phenotypic analysis of rice ZH11 seedlings under different NaCl treatments for one week. A, Representative phenotypes of rice seedlings treated with three NaCl concentrations (0.125%, 0.25%, and 0.5%) compared with control (CK, H_2O); B, Quantitative analysis of phenotypic traits, including primary root length, lateral root length, shoot length. Asterisks indicate statistically significant differences based on one-way ANOVA (ns: not significant, *P < 0.05, **P < 0.01).

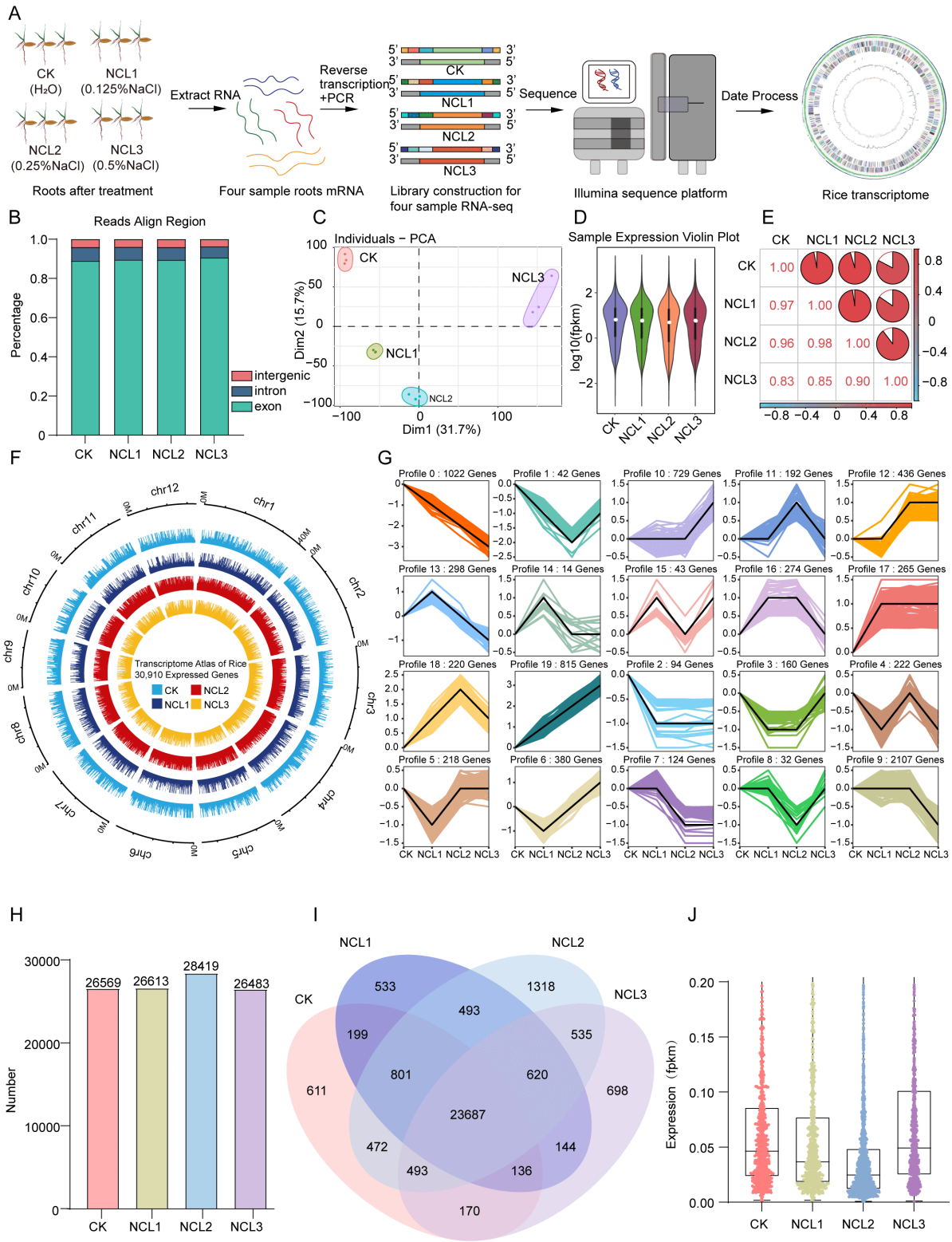


Figure 2

Overview of transcriptomic data quality and gene expression patterns in salt treated ZH11 rice seedlings. A, Schematic diagram of transcriptome library construction; B, Summary of read mapping statistics; C, principal component analysis of all samples under different treatments; D, Violin plot showing the distribution of gene expression levels; E, sample correlation heatmap; F, Genome-wide distribution of expressed genes across 12 rice chromosomes; G, K-means clustering of gene expression

profiles; H, total number of expressed genes in each treatment group; I, Venn diagram showing shared and unique genes among treatments; J, Gene expression level distribution across samples.

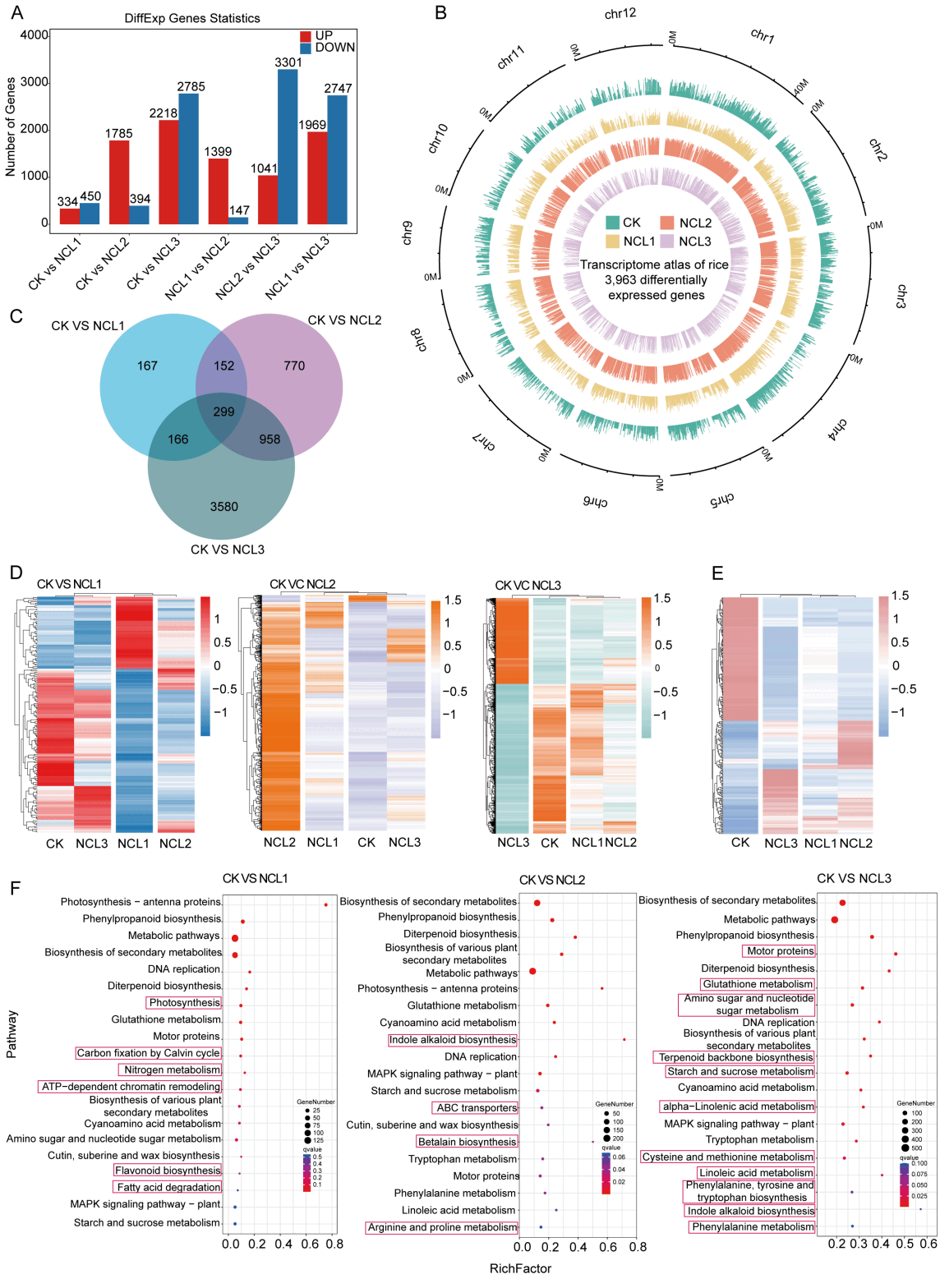


Figure 3

Identification and functional analysis of differentially expressed genes in rice ZH11 young roots under NaCl treatments. A, Summary of upregulated and downregulated DEGs across different comparisons; B,

Circos plot showing chromosomal distribution and expression patterns of DEGs; C, Venn diagram illustrating shared and unique DEGs among CK vs NCL1, CK vs NCL2, and CK vs NCL3 comparisons; D, Heatmap of group-specific DEGs; E, Heatmap showing expression patterns of 299 common DEGs; F, KEGG pathway enrichment analysis of DEGs under different salt concentrations.

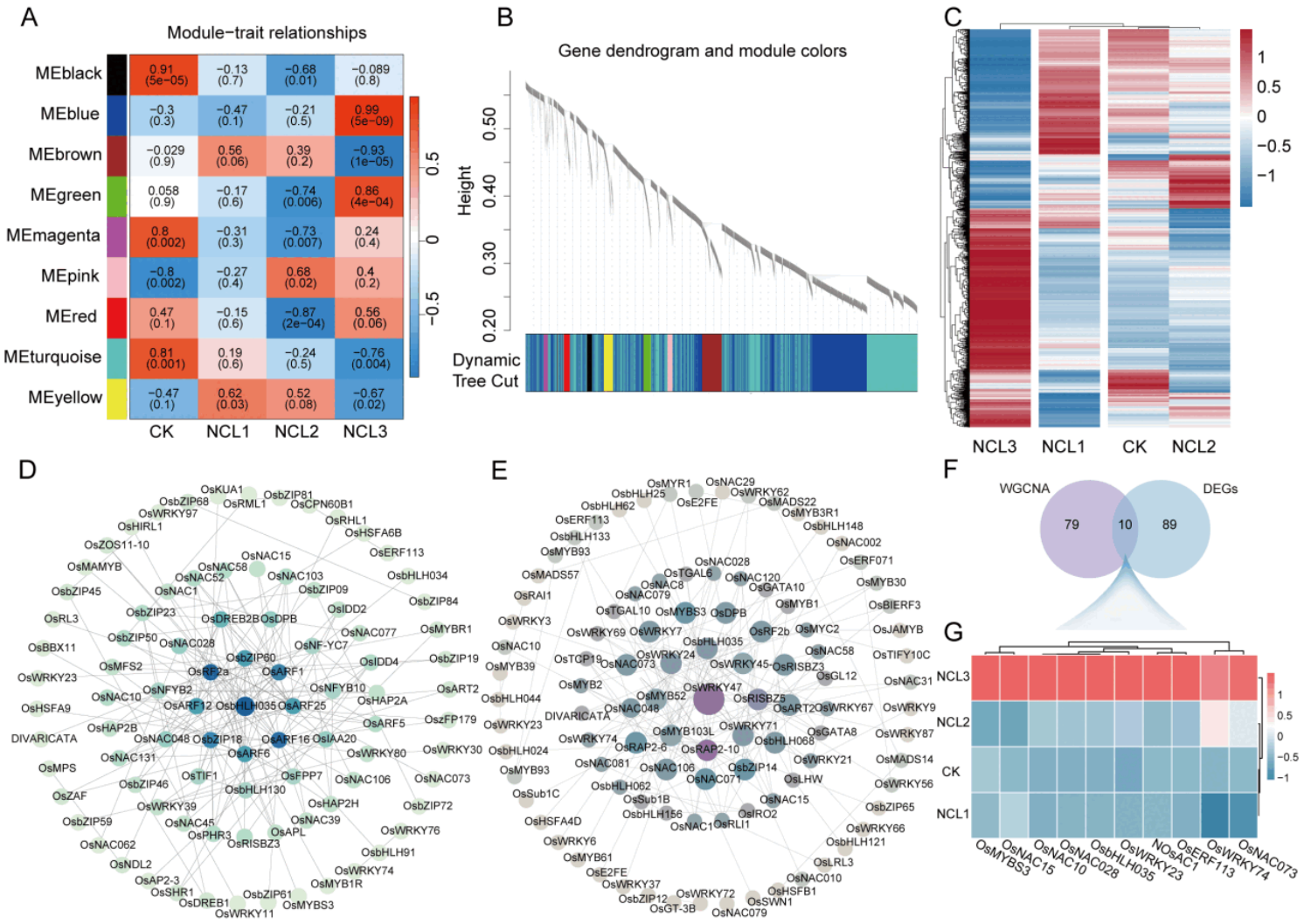


Figure 4

Integrated analysis of gene co-expression modules, functional enrichment, and transcription factor regulatory networks in rice under salt stress. A, Module trait relationship heatmap showing correlations between gene co-expression modules and salt treatments; B, Gene dendrogram and module identification based on hierarchical clustering; C, Expression heatmap of key module genes identified by WGCNA; D, Co-expression network highlighting hub genes within core modules; E, Network analysis of transcription factors associated with DEGs; F, Venn diagram showing overlap between transcription factors identified by WGCNA and DEGs; G, Expression heatmap of ten overlapping key transcription factors under different treatments.

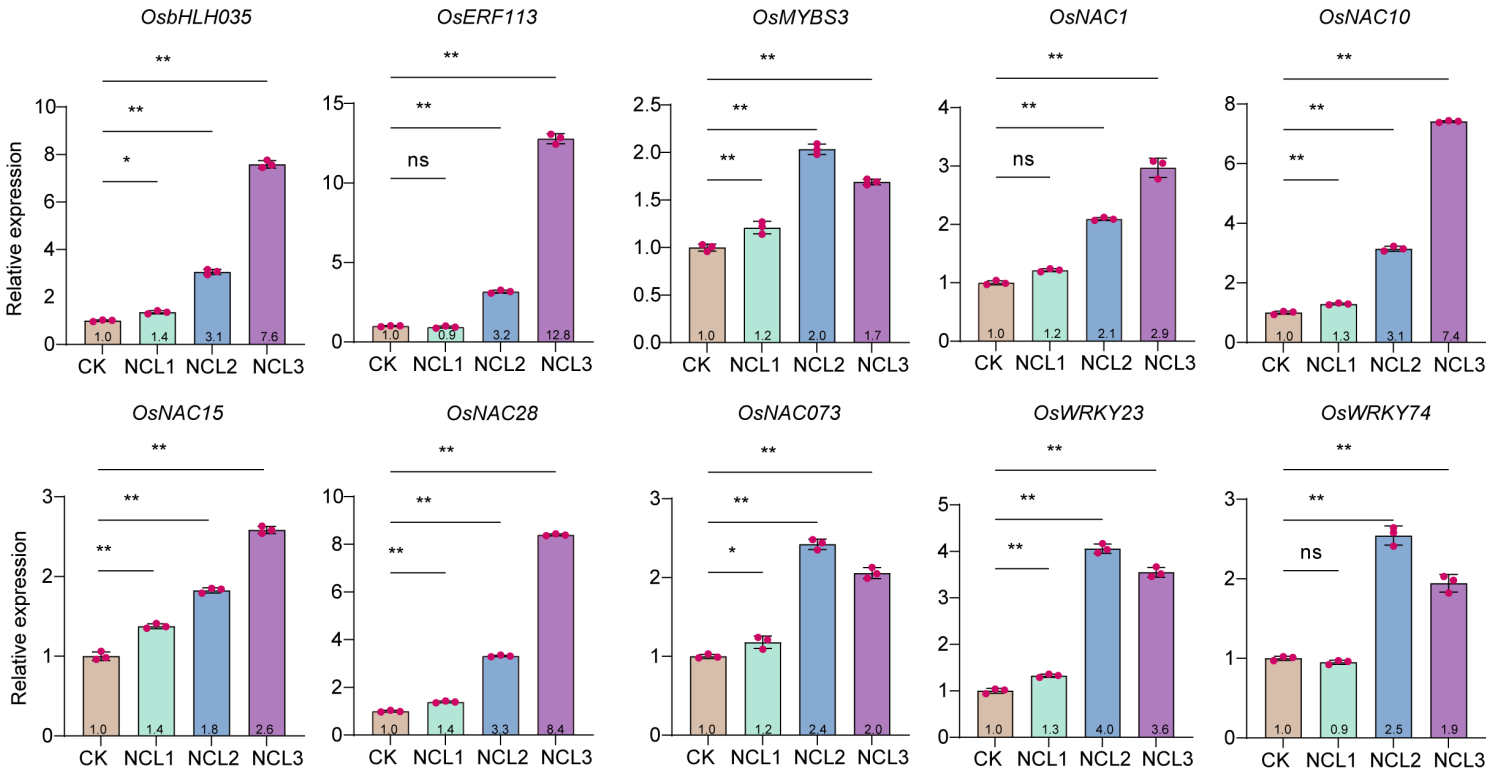


Figure 5

RT-qPCR validation results of salt stress responsive transcription factors in rice under NaCl treatments. Relative expression levels of selected transcription factors under different NaCl concentrations. Asterisks indicate statistically significant differences (ns: not significant, *$P < 0.05$, **$P < 0.01$).

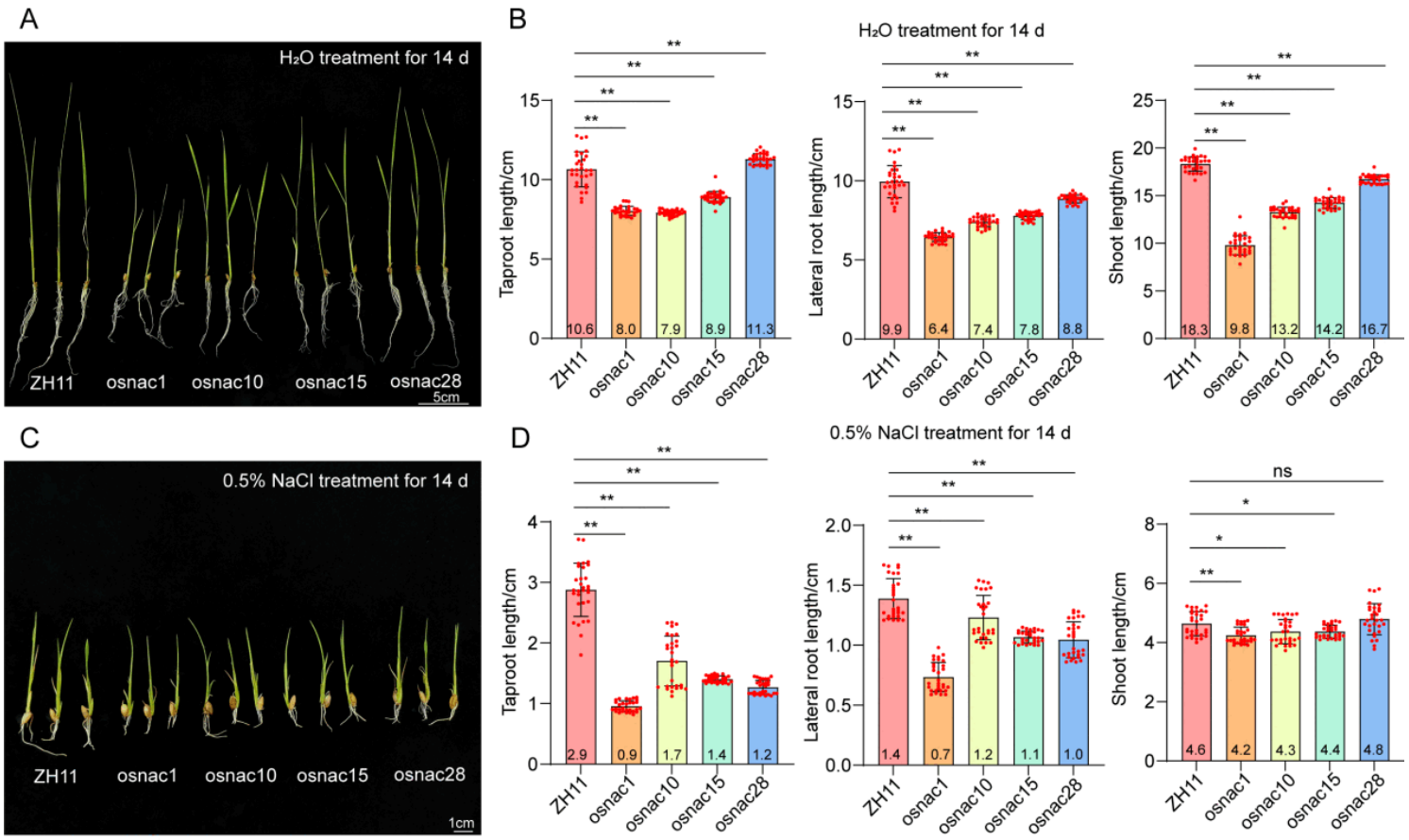


Figure 6

Phenotypic analysis of NAC family mutants in rice under control and salt stress conditions. A, Representative seedling phenotypes under H_2O for 14 days; **B**, Quantitative measurements (primary root length, lateral root length, and shoot length) under H_2O for 14 days; **C**, Representative seedling phenotypes under 0.5% NaCl for 14 days; **D**, Quantitative measurements (primary root length, lateral root length, and shoot length) under 0.5% NaCl for 14 days.

Supplementary Files

This is a list of supplementary files associated with this preprint. Click to download.

- figureS.zip
- tableS.zip